

# Design of a High Power 10-KW Solid-state Heat Capacity Laser and the Thermal Management

Hasan Ebadian\*, Mohammad Mahdi Moslem, and Nabiollah Azarpoor

Faculty of Applied Sciences. Malek Ashtar University of Technology, Iran

Corresponding author email: [morebady@yahoo.com](mailto:morebady@yahoo.com)

Received: Nov. 11, 2024, Revised: Jan.6, 2024, Accepted: Jan. 10, 2024, Available Online: Jan. 12, 2024  
DOI: 10.61186/ijop.17.1.47

**ABSTRACT**— The simulation results of a 10-kW heat capacity slab laser are presented. Two different schemes for optical pumping with high-power laser diodes are investigated. The simulation of optical pumping using ZEMAX software demonstrates a uniform pump distribution within the laser slabs. Additionally, the temperature distribution in the laser slab is examined using COMSOL. The findings for two distinct laser designs reveal that increasing the slab dimensions reduces the temperature distribution and thermal issues. Furthermore, cooling schemes indicate that the cooling phase of a 10-kW HCL falls within the range of 20-40 seconds. A comparison of water and air cooling of the optically pumped slabs during the cooling phase demonstrates that water cooling is more efficient than air cooling. The simulation results confirm that the proposed laser will be an efficient device for laser material processing. A focused 10-kW HCL laser will melt the steel sheet after less than 1 s at 1490 K.

**KEYWORDS:** COMSOL, cooling phase, gain, Heat Capacity Laser, Nd:YAG ceramic, solid-state, temperature distribution,

## I. INTRODUCTION

The subject of this work is the study of solid-state lasers, especially thermal capacity lasers or Heat Capacity Lasers (HCL). In fact, solid-state lasers are one of the oldest types of lasers. However, due to their advantages over other types of lasers, research and innovation in these lasers continues. Although solid-state high-power lasers may not be economically viable compared to other existing lasers at first glance, but due to the wide range of laser activities and

the existence of areas that need special equipment, the importance of solid-state lasers has not decreased, but the value of solid-state lasers has become more apparent than before.

It is important to note that solid-state lasers are used in specialized applications, such as military and medical. Thermal capacity lasers are even more specialized and have been developed for military applications. In terms of research and development, there is a limited amount of work done on thermal capacity lasers compared to solid-state lasers. In fact, only a few research institutions around the world have conducted research on this topic, and the results have been made available to the public in a limited way. One of the humanitarian applications of HCL lasers is their use in the field of mine clearance. This system can clear both surface and buried mines by operating at a safe distance from them. In the case of high-risk explosive materials, this system can cut them in place and prevent the threat of explosion to humans. Laser material processing is another application of high-average-power solid-state lasers [1].

There are different methods to produce high-power solid-state lasers. In 1960, after the invention of the first solid-state laser, the development and optimization of various types of lasers began, and various laser theories were proposed. Soild-state disk laser based on Nd:YAG active medium, is one of the approaches. High power thin disk lasers were widely investigated and different aspects was

considered [2]-[4]. Also, the multi-slab high power solid-state laser was under investigation [5]. The rules of power scaling of high-power solid-state slab lasers was investigated by few research groups [6, 7].

Compared with conventional cooling operation, the heat capacity operation mode can be divided into two periods: lasing period and cooling period. In the lasing phase, heat is accumulated in the active medium without cooling. At the end of the lasing phase, the pump source is turned off and the cooling phase begins. In a short time, the temperature of the active medium returns to its initial value. This pumping arrangement is like a single-shot pumping arrangement that is repeated regularly, with effective cooling designed for the active medium between shots [8].

In fact, in the 1990s, the Lawrence Livermore National Laboratory (LLNL) began to develop a new type of compact laser and proposed the theory of thermal capacity lasers in this time period. So far many groups have investigated different aspects of SSHCL [9-13]. The Rotter group worked on a SSHCL with a 13cm aperture Nd: GGG (Nd doped Gadolinium Gallium Garnet) gain medium, they could get 10 KW output power. Also it was verified that, by increasing the active media aperture and reducing the slab quantity, it is possible to get the same energy per pulse from the laser system. Moreover, the results of beam quality control in SSHCL was published by different groups. The technical challenges for high energy lasers was considered and adaptive optics control system was installed in the laser system to control the laser beam quality [14].

In 2001, the first prototype of a thermal capacity laser with a flash lamp pumping source and Nd:Glass active medium was built with the aim of scientifically proving the theoretical grounds proposed for thermal capacity lasers. This laser device was built by the LLNL with an average output power of 13 kW or energy of 500 to 1000 Joules per pulse at a repetition rate of 20 Hz. This output power with a simple structure used in the laser design was a

scientific proof for the thermal capacity method.

It has been proven that transparent ceramic Nd:YAG laser materials can operate at temperatures up to 200°C without cracking or sustaining physical damage. However, the operating time is limited to 10 seconds due to thermal limitations [1]. Experimental results indicate a temperature rise of approximately 0.05 K per pulse. Therefore, at a pulse repetition rate of 200 Hz, the temperature will rise by about 100 K. In this study, we will consider a HCL system with a pulse repetition rate of 200 Hz and a lasing time of 10 seconds [1]. Temperature analysis and control in heat capacity lasers were carried out theoretically and experimentally [15-17]. Also, other types of gain mediums based on HCL, was considered and studied numerically and experimentally [21,22]

This work investigates the design procedure of a Solid-State Heat Capacity Laser (SSHCL) with 10 KW output power based on a transparent Nd:YAG ceramic active medium. The simulation results for energy extraction and gain medium parameters for an Nd:YAG gain medium are presented. Additionally, the details of ray tracing simulations for two pumping modules are considered and analyzed. The temperature limitations for two high-average-power SSHCLs are investigated in more details using COMSOL simulation software, and the best operating conditions for the lasing and cooling phases are extracted. Additionally, the simulation results for laser-material interaction of a HCL output laser with a steel sheet will be presented.

## II. THEORETICAL REVIEW

### A. *Optical pumping considerations and gain medium*

To gain an initial understanding of the subject, it is necessary to briefly study the power and optical pumping of the gain medium issues in solid-state lasers. First, the power extraction relationships will be considered, followed by the temperature-dependent problems.

Solid-state slab structures are well-suited for high-power multi-kilowatt laser systems because power scaling is easier compared to rod geometry due to the modified thermal problems associated with zig-zag propagation in the laser.

Figure 1 shows the optical pumping structure of a Nd:YAG solid-state laser. Each pump module consists of four two dimensional (2D) stacks that provide uniform radiation power in the gain medium's absorption band at 808 nm (the 2D arrays are lensed for Fast Axis Collimation with slow axis divergence of 10 degrees and fast axis collimation of 0.5 degrees). The laser diode radiation is oriented to create a uniform pump distribution throughout the slab volume. This pumping structure is then placed inside a laser resonator. Optical pumping with suitable two-dimensional laser diodes excites the laser medium and initiates the laser process.

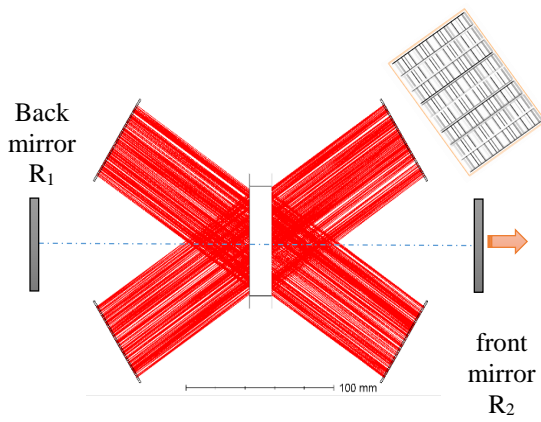


Fig. 1. The schematic diagram of an optically pumped laser slab, installed in a laser resonator

To calculate the amount of optical power required to achieve 10 kW, it is necessary to first theoretically analyze the governing relationships of this process and then predict the output power using an engineering design process. The basic structure of a HCL is the laser gain module, which consists of a slab-geometry gain medium and two-dimensional high-power laser diode arrays on both sides of the laser slab.

Two extended surfaces of the slab are pumped at special angles to achieve uniform optical pump distribution across the slab face. In this work, Nd:YAG slabs are pumped by high-

power diode laser stacks in quasi-continuous wave (QCW) mode of operation. The pump power distribution results by ZEMAX is shown in Figs. 2 and 3. In the all simulations of this work, two high power laser diode sources is considered: 5 KW and 10 KW.

The pump laser diode is divided into two distinct sources at each face of the slabs (for example, the 5 kW source consists of two 2500 W stacks at each face of the slabs).

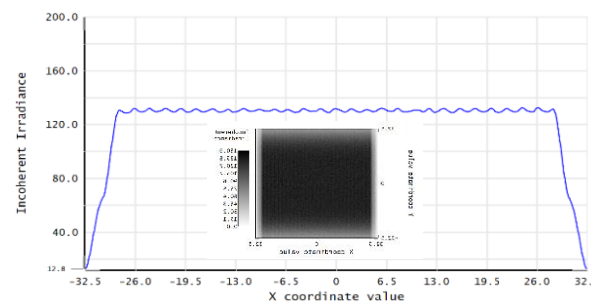


Fig. 2. The pump intensity distribution ( $\text{W}/\text{cm}^2$ ) vs. slab thickness for design#1 slabs with 2500W optical pumping from each side (inset: the pump distribution in the slab faces)

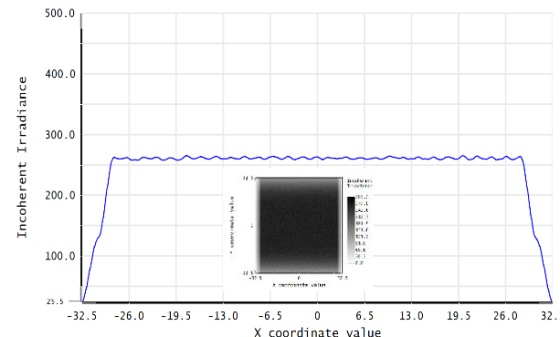


Fig. 3. The pump intensity distribution ( $\text{W}/\text{cm}^2$ ) vs. slab thickness for design#2 slabs with 5000W optical pumping from each side (inset: the pump distribution in the slab faces).

As mentioned before, the temperature behavior of the slab, plays an important role in HCL laser systems. One important consideration is the gain medium's ability to withstand the high temperature gradients during pumping and lasing conditions. Nd:YAG crystals are common laser materials for high-power laser systems, but beam quality considerations limit their use. Other laser gain mediums, such as Nd:GGG, are widely used in SSHCL laser systems. New laser materials with optical and

laser characteristics similar to Nd:YAG are currently under development.

Polycrystalline Nd:YAG ceramic laser materials have been investigated for HCL lasers since 2006. Konoshima Company has developed these gain media, and LLNL has installed them in the 67 kW high-power HCL laser system [18].

Transparent Nd:YAG laser ceramics have the same optical parameters as crystals, but modified mechanical parameters. Table 1 compares two types of laser active media with crystal and ceramic production methods. The thermal fracture limit of laser crystals increases with the active ion doping level, but in laser ceramics it is possible to increase the doping concentration to 0.5-4% without sacrificing fracture strength. An important parameter that is similar for YAG crystals and ceramics is thermal conductivity. Ueda experimentally show that this parameter is the same for both materials:  $K_{\text{crystal}} = 10.5 \pm 0.5$ ,  $K_{\text{ceramic}} = 10.7 \pm 0.5$  (W/mK) [19].

Table 1. Comparison of two laser materials [19]

material	Nd:YAG Crystal	Nd:YAG Ceramics
$\sigma$ (cm <sup>2</sup> )	$3 \times 10^{-20}$	$3 \times 10^{-20}$
$\tau$ (μs)	260	260
$\sigma\tau$ product (cm <sup>2</sup> s)	$7.8 \times 10^{-23}$	$7.8 \times 10^{-23}$
Fracture limit (MPa)	1.8	5.2
Mass production	No	Easy
Possible cost	High	Medium
$\alpha$ (1/K)	$7.8 \times 10^{-6}$	$7.8 \times 10^{-6}$

## B. Gain considerations

Each HCL consists of  $n$  slabs with the same dimensions, confined between two laser resonator mirrors. The laser resonator has a total length of  $L$  and back and front mirror reflectivity of  $R_1$  and  $R_2$ , respectively. The total efficiency of the laser system,  $\eta_{\text{sys}}$ , which is the product of different efficiencies, can be calculated by using Eq. 1 [20]:

$$\eta_{\text{sys}} = \eta_{\text{abs}} \eta_t \eta_Q \eta_s \eta_B \quad (1)$$

where  $\eta_{\text{abs}}$ ,  $\eta_t$ ,  $\eta_Q$ ,  $\eta_s$ ,  $\eta_B$ , and  $\eta_c$  are: absorbtion, transfer, quantum, stocks, beam overlap, and coupling efficiencies, respectively. Another important parameters that need to be

calculated for the laser output energy per pulse are well known as the small signal gain,  $g_0$ , and the threshold power,  $P_{\text{th}}$  that are given by the Eqs. (2) and (3) [20]:

$$g_0 = \sigma \tau_f \eta_{\text{sys}} p_{\text{in}} / h \nu_l V \quad (2)$$

$$P_{\text{th}} = \left( \frac{\delta - \ln R}{2} \right) \frac{A h \nu_l}{\eta_{\text{sys}} \sigma \tau_f} \quad (3)$$

where  $\sigma$  is the stimulated emission cross section,  $\tau_f$  is the fluorescence life time,  $p_{\text{in}}$  is the laser diode optical power,  $h \nu_l$  is the 1064nm photon energy,  $V$  is the gain medium volume,  $\delta$  is the total resonator loss,  $R$  is the output coupler reflectivity,  $A$  is the gain medium cross section and  $\eta_{\text{sys}}$  is the total system efficiency.

The output power of a HCL system,  $P_{\text{out}}$ , with the temperature of the active medium  $T$ , assuming that the pump has an uniform distribution, can be calculated analytically by using Eq. (4) [8]:

$$P_{\text{out}} = \frac{P_{\text{heat}} \eta_{\text{extr}}}{\chi} - V P_{\text{th}} D_t \eta_{\text{extr}} = \left[ \frac{P_{\text{heat}} \eta_{\text{extr}}}{\chi} - \frac{V h \nu_n \exp(-E_{\text{ll}}/kT)}{\tau_{\text{life}}} \right] \quad (4)$$

where  $P_{\text{heat}}$  is the heat power,  $\eta_{\text{extr}}$  is the extraction efficiency that is generally about 0.5.  $\tau_{\text{life}}$  is the upper laser level lifetime and the parameter  $E_{\text{ll}}/kT$  is the population of the lower laser level,  $D_t$  is duty cycle and  $\chi$  is the heating parameter. The heat deposited during the optical pumping and lasing process is calculated by [8]:

$$P_{\text{heat}} = \frac{2 P_{\text{pump}}}{w} \eta_{\text{abs}} V \frac{\chi}{1+\chi} \quad (5)$$

where  $w$  is the slab width,  $\eta_{\text{abs}}$  is the absorbtion efficiency and  $P_{\text{pump}}$  is the optical laser diode pumping power at 808nm. Moreover, the temperature increase during lasing phase is given by [8]:

$$\Delta T = \frac{P_{\text{heat}}}{m C_p(T)} \quad (6)$$

where  $t$  is time of heat deposition and  $m$  is the slab mass under optical pumping.

### C. Temperature Distribution in a HCL Slab

Heat transfer in solid-state lasers poses a significant challenge in laser system design. In the slab geometry of the SSHCL gain medium, various methods exist for removing heat from the gain medium during the cooling phase. Typically, SSHCL systems operate in QCW mode with high repetition rates and long pulse durations (e.g., 200 Hz and 500 microseconds) for approximately 10 seconds. Subsequently, optical pumping ceases, and the cooling phase of the hot slab commences, which may require several seconds to cool down to the initial temperature. An intriguing scheme for slab cooling involves forced convection of water flowing in a narrow channel to dissipate heat from the high-temperature slab's surface.

Utilizing COMSOL software, this study investigates the temperature distribution in an HCL laser system under various conditions. We examine two slab laser geometries: design#1 and design#2, with dimensions of 40mm×40mm×10 mm and 65mm×65mm×15 mm, respectively. The optical pumping and slab parameters are presented in Table 2.

Table 2. The COMSOL simulation parameters

Parameter	Design#1	Design#2
Slab dimensions (mm <sup>3</sup> )	40×40×10	65×65×15
P <sub>pump</sub> for each slab (W)	5000	10000
Duty cycle (%)	10	10
Lasing time (s)	10	10
Cooling time (s)	1-60	1-60
Cooling scheme	water	water
Cooling temperature	variable	variable

### D. Simulations

The implemented model for the 10-kW HCL laser under investigation is depicted in Fig. 4. The laser medium comprises  $N$  slabs, each with a thickness of  $t$ , positioned between two laser resonator mirrors. The total gain medium thickness is given by  $L_{\text{slab}}=Nt$ . Each slab face is subjected to laser diode pumping with sufficient power intensity.

The simulation study encompasses two distinct phases: lasing and cooling. During the lasing phase, the slab is pumped by high-power 2D laser diode stacks for 10 seconds. Subsequently, the pump is turned off, and the cooling phase commences. The cooling phase persists until the slab attains ambient temperature, employing two distinct cooling schemes discussed earlier.

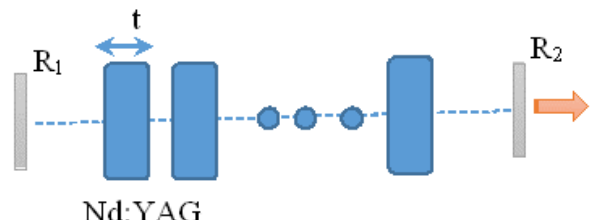


Fig. 4. the implemented model for high average power Nd:YAG ( $R_1$  and  $R_2$  are the back and output mirror reflectivities)

### E. Lasing phase

In this section, the output power of the high-power HCL laser is calculated using Eqs. (1-6). Table 3 presents the initial and calculated parameters utilized for output power simulations. The HCL under investigation is a high average power 10-kW slab laser system. Simulations were carried out for the two aforementioned slabs, design#1 and design#2, with two different optical pumping powers: 5000 W and 10000 W, respectively. The output power simulation results for the two designs are displayed in Table 4.

Table 3. The simulation parameters for 10-kW HCL

Parameter	Value
Optical to optical efficiency [7]	~ 20%
$\eta_{extr}$	0.5
YAG density (gr/cm <sup>3</sup> )	4.6
$C_p$ (J/gr K)	0.58
$\eta_{abs}$	0.75
$\eta_t$	0.85
$\eta_B$	0.80
$\chi$	0.3
Output mirror reflectivity	30%

To investigate the impact of symmetric optical pumping from opposite sides of the slabs, a line graph was extracted using COMSOL. The simulation results for design#2 under 10000 W optical pumping power are presented in Fig. 5.

We think that the design#1 also will exhibit similar behavior.

During the lasing phase, evaluating the temperature behavior of the slab under high-intensity optical pumping is informative. For two slabs, design #1 and design #2 with 10000 W optical pump power, the temperature distribution is shown in Figs. 6 and 7 for 10 s lasing periods. The maximum temperatures of slabs at design #1 and design #2 are 375 K and 395 K, respectively. These simulation results align closely with those reported by Hou [16].

Table 4. The HCL output power for two designs

Gain medium	design#1	design#2
Total optical pump power (W)	50000	50000
Threshold power (W)	1570	4200
N (number of slabs)	10	5
Output power (W)	12400	11500

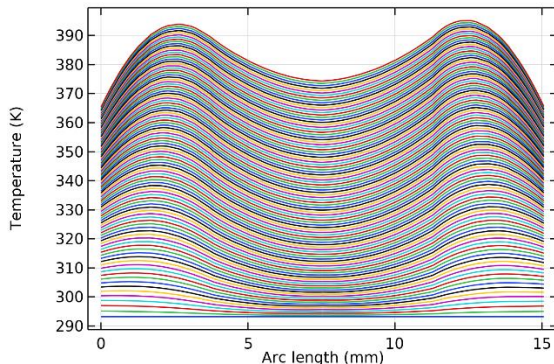


Fig. 5. The line graph of pumped design#2 under symmetric optical pumping.

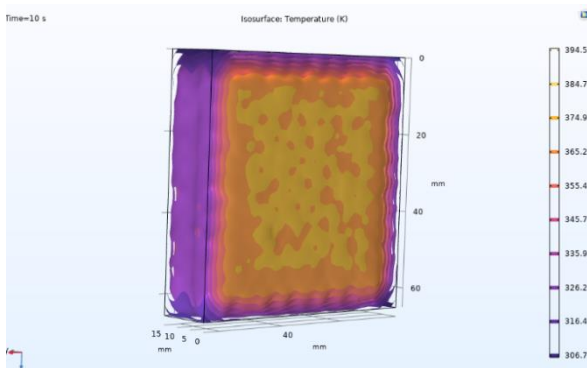


Fig. 6. Temperature distribution in the 5000 W pumped laser design#1(the maximum temperature is about 375 K)

## F. Cooling phase

This section delves into the cooling phase of the HCL system. Cooling commences abruptly following the onset of laser operation. Two distinct cooling methods were considered in this investigation: water cooling and forced air cooling.

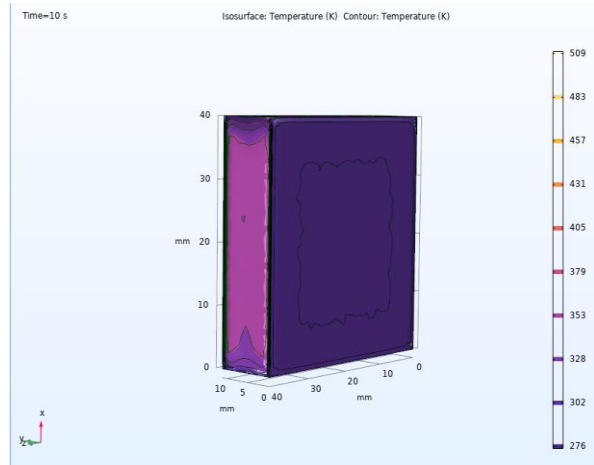


Fig. 7. Temperature distribution in the 10000 W pumped laser design#2. (The maximum temperature is about 395 K)

In the case of water cooling, the optical pumping is abruptly terminated after a 10-second lasing phase, and the cooling phase commences by directing the coolant onto the slab surfaces. The heat removal from the slab surface leads to a reduction in the temperature of the pumped slabs. The cooled slab temperature at different time intervals is presented in Fig. 8 for design#2.

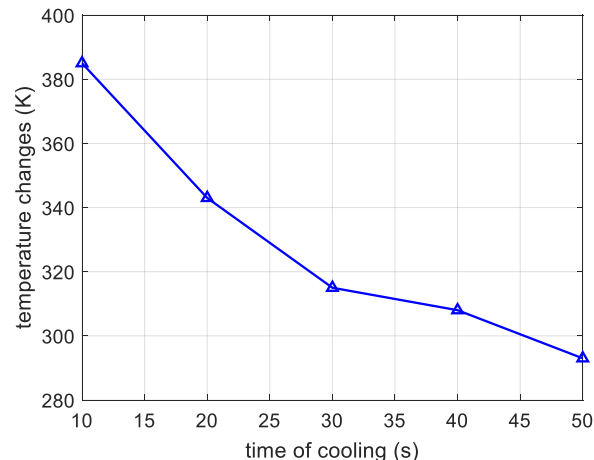


Fig. 8. Time depended temperature reduction of the slab at cooling phase (design #2).

The next step of the simulations explored the effect of cooling temperature on the cooling phase recovery time. Three coolant temperatures were chosen: 273, 283, and 293 K with the flow velocity of 66 mm/s. The simulation results for both design #1 and #2 are shown in Figs. 9 and 10.

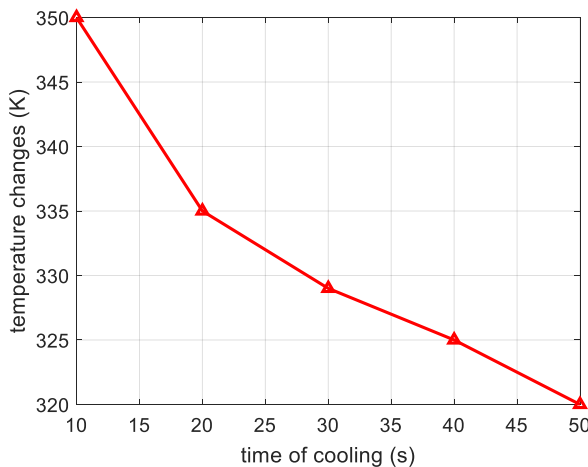


Fig. 9. The effect of various temperature cooling on slab temperature recovery in cooling phase for design #1.

### G. Air cooling scheme

Investigating alternative cooling schemes, such as air cooling, which is widely employed in various high-energy lasers, is of paramount importance. Cryogenic cooling, for instance, is a suitable method for cooling hot laser active materials.

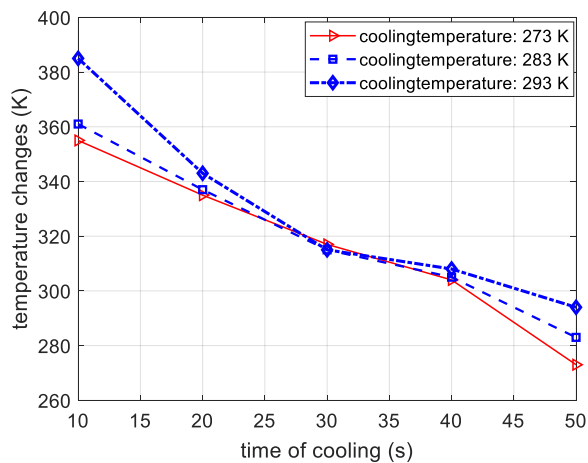


Fig. 10. The effect of various temperature cooling on slab temperature recovery in cooling phase for design #2.

In this study, we examined the air cooling of pumped slabs (design #1) during the cooling phase of the HCL. The cooling agent is a cold

air (nitrogen) stream at 100 K. The initial temperature of the pumped slab after 10 s was approximately 379 K. The simulation results at time steps of 10 seconds are shown in Fig. 11. It is evident that the slab in the cooling phase could not return to its initial temperature after 50 s. The temperature drops by only 15 K after 30 s of cooling time. The lower heat transfer rate of air cooling compared to water cooling can be attributed to the lower convection heat transfer coefficient of air. The temperature distribution of the slab under cooling phase for cooling times of 10 and 50 s is shown in Figs. 12(a) and 12(b).

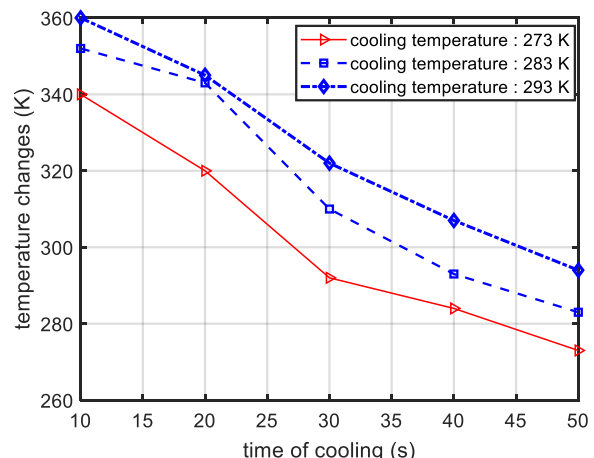
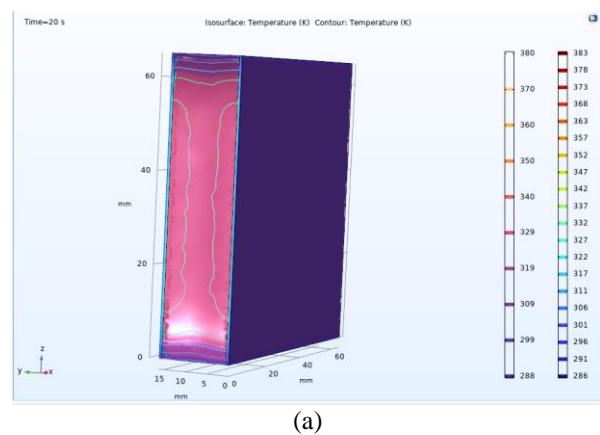


Fig. 11. The simulation results of air-cooled slab in the cooling phase for design #1.



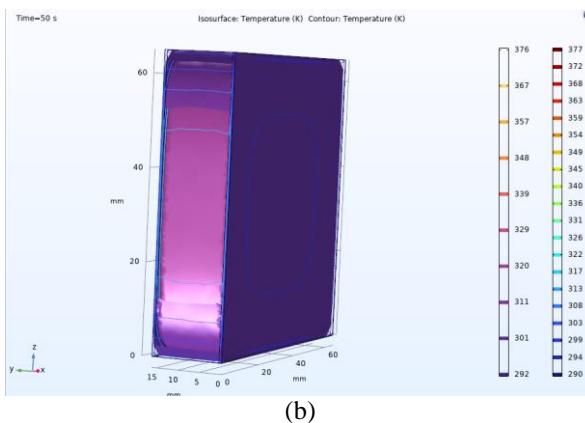


Fig. 12. Cooling phase of the slab by cold air after (a) 20s and (b) 50s.

## H. Laser material interaction

In this section, to evaluate the ability of the HCL system for some applications, we explored the impact of focused HCL spot on a 1 mm thick steel sheet. The thermal properties of the steel and the focused laser parameters are presented in Table 5. The simulation results indicate that the metal will begin to melt due to the high laser power input and reaching its melting point (Fig. 13). Consequently, the 10-kW laser system is expected to be an efficient device for laser material processing under specific conditions.

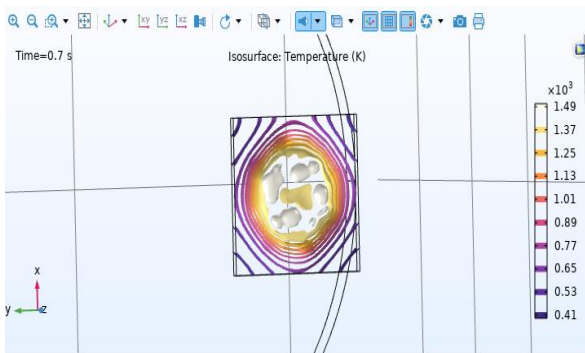


Fig. 13. The simulation results of laser interaction with a steel sheet. The temperature in the focus is about 1490 K

From Fig. 13 it can be understood that the high temperature at the focused point of the laser, is capable to melt various metals like Al, Brass, copper, cast iron and so on. Moreover, the further simulation show that, after about 0.7 s, the melting conditions is meet and the temperature is approximately constant for next times (Fig. 14).

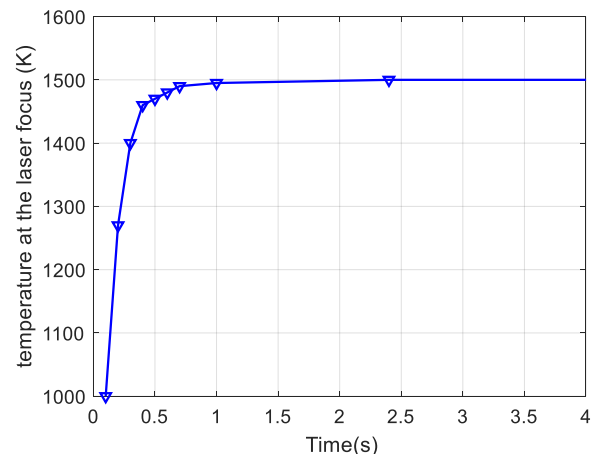


Fig. 14. The focus spot temperature change Vs time evolution

Table 5. Physical Properties of Steel

Specific Heat Capacity(J/g·°C)	0.5
Thermal Conductivity (W/m·K)	16.2
Melting Point (°C)	1200
Liquidus (V)	1455
Laser power(W)	10000
Laser spot size (mm)	5

## III. CONCLUSION

In conclusion, this work investigated and simulated the design parameters of a high average power SSHCL with a 10 kW output power. The simulation encompasses both the power and temperature behavior of such systems, which are intrinsically linked and temperature-dependent. Simulations reveal that extracting 10 kW power from an HCL system necessitates careful consideration of the slab dimensions and temperature removal during the two successive phases (lasing and cooling). Two different slabs with dimensions of 6 cm × 6 cm × 1.5 cm and 4 cm × 4 cm × 1 cm were considered and pumped with high-power 2D laser diode stacks. The system is optically pumped for 10 s, followed by a cooling phase. It was concluded that increasing the slab dimensions and optical pumping power does not lead to a significant increase in the slab temperature. Moreover, the simulations demonstrate that for the same output energy, the number of 4 cm × 4 cm slabs is twice that of 6 cm × 6 cm slabs. The simulations reveal that the cooling phase is approximately three to four times longer than the lasing phase. This will limit the firing rate of the system. Under such conditions, it is proposed to replace the hot

slabs with low-temperature slabs and cool them in a rotating slab manner. Furthermore, the laser-material interaction simulation for a steel sheet and high-power HCL laser indicates that the investigated laser will be efficient for steel cutting and metal welding applications.

## REFERENCES

[1] H. Injeyan and G. Goodno, *High-Power Laser Handbook*, Mc Graw- Hill, p. 277, 2010.

[2] H. Aminpour, A. Hojabri, M. Esmaeili, I. Mashaiekhy Asl, "Investigation of absorption pump light distribution in edged-pumped high power Yb:YAGYAG disk laser," *Int. J. Opt. Photon.*, Vol. 5, pp. 49-56, 2011.

[3] H. Amin Pour, Alireza Hojabri, "Performance Simulation of Side-Pumped Slanted Faces of High Power Yb:YAGYAG Thin-Disk Laser," *Int. J. Opt. Photon.*, Vol. 6. pp. 31-40, 2012.

[4] I. Rahmani and M. Ghanaatshoar, "Influence of Laser Pulse Energy on CFTS Thin Film Deposited by Pulsed Laser Deposition," *Int. J. Opt. Photon.*, Vol. 16. , pp. 131-138, 2022.

[5] X. Fu, Q. Liu, P. Li, L. Huang, and M. Gong, "Numerical simulation of 30-kW class liquid-cooled Nd:YAG multi-slab resonator" *Opt. Exp.*, Vol. 15, pp. 18458-8470, 2015.

[6] S.T. Rutherford, W.M. Tulloch, E.K. Gustafson, and R.L. Byer, "Edge-Pumped Quasi-Three-Level Slab Lasers: Design and Power Scaling," *IEEE J. Quantum Electron.*, Vol. 36, pp. 205-219, 2000.

[7] S. Zhang, S. Zhou, X. Tang, G. Bi, and H. Lu, "Investigation of laser diode face-pumped high average power heat capacity laser," *Chin. Opt. Lett.* Vol. 4, pp. 658-660, 2006.

[8] G.F. Albrecht, S.B. Sutton, EV. George, W.R. Sooy, and W.F. Krupke, "Solid-state heat capacity disk laser", *Laser Particle Beams*, Vol. 16, pp. 605-625, 1998.

[9] M.D. Rotter, C.B. Dane, S.A. Gonzales, R.D. Merrill, S.C. Mitchell, C.W. Parks, and R.M. Yamamoto "The Solid-State Heat-Capacity Laser," *Advanced Solid-State Photonics* Santa Fe, New Mexico, pp. 1-4, 2004.

[10] R. Yamamoto, J. Parker, C. Boley, K. Cutter, S. Fochs, A. Rubenchik, "Laser-Material Interaction Studies Utilizing the Solid-State Heat Capacity Laser," *20th Annual Solid-state and diode Laser Technology Review*, May 9, 2007.

[11] G. Ming-Xiu, L. Jin-Dong, F. Wen-Qiang, S. Xiang-Chun, H. Qi-Quan, and C. Wei-Biao, "A Kilowatt Diode-Pumped Solid-State Heat-Capacity Double-Slab Laser," *Chin. Phys. Lett.*, Vol. 23, pp. 2530-2533, 2006.

[12] Y. Dong, J. Zu, L. Hou, X. Yin, T. Zhang, Y. Gu, Z. Liu, and J. Zhu, "Approximate formulas of temperature and stress distributions and thermal induced effects in a heat capacity slab laser," *Chin. Opt. Lett.*, Vol. 4, pp. 326-328, 2006.

[13] M. Eichhorn, "High-efficiency multi-kilowatt  $Er^{3+}$ :YAG solid-state heat-capacity laser," *Opt. Lett.*, Vol. 36, pp. 1245-1247, 2011.

[14] K.N. LaFortune, R.L. Hurd, S.N. Fochs, M.D. Rotter, P.H. Pax, R.L. Combs, S.S. Olivier, J.M. Brase, and R.M. Yamamoto, "Technical challenges for the future of high energy lasers," *Proc. of SPIE Vol. 6454*. pp. 645401-6454011, 2007.

[15] J. YANG, X. WAN, X. XU, and Q. LU, "Analysis and Experimental Study of the Temperature and Stress Distribution in the Slab of Solid-State Heat Capacity Laser," *Proc. of SPIE*, Vol. 6622, pp. 66221I-1, 2007.

[16] L. Hou, J. Zu, Y. Dong, X. Yin, and J. Zhu, "Numerical Analysis on the Cooling Characteristics of Finite Nd: GGG Slab in a Solid-State Heat Capacity Laser," *Proc. of SPIE Vol. 6279*, pp. 62796U-1, 2007.

[17] Y. Dong, J. Zu, L. Hou, Z. Liu, X. Yin, and J. Zhu, "A potential method to control thermal distribution in a solid-state heat capacity laser, *Proc. of SPIE Vol. 6279*, pp. 6279U1-7, 2007.

[18] R.M. Yamamoto, B.S. Bhachu, K.P. Cutter, S.N. Fochs, S.A. Letts, C.W. Parks, M.D. Rotter, and T.F. Soules, "The Use of Large Transparent Ceramics in a High Powered, Diode Pumped Solid-State Laser," *Advanced Solid-State Photonics*, Japan, WC5, 2008.

[19] K. Ueda "Recent Progress of Ceramic Laser for Ultrashort Pulse Lasers," *Inst. Laser Science, Univ. Electro-Communications, ICUIL-China*. 2008.

[20] W. Koechner, *Solid-state laser engineering*, 6<sup>th</sup> Ed., Springer, 2006.

[21] Y.-L. Wang and S.-P. Chen, "Numerical simulation of thermal distribution in quasi-

heatcapacity fiber lasers," IOP Conf. Ser Earth Environ. Sci. Vol. 565, 2020.

[22] JIA Guan-nan, Y. Shun, G. Xiang-yu, and L. Tian, "Transient Thermal Characteristics of Heat Capacity High Power Diode Lasers," Chin. J. Luminescence, Vol. 37, pp. 422-427, 2016.



**Hasan Ebadian** was born in 1975. He received his PhD degree in Atomic and Molecular Physics from Rafsanjan University, Kerman, Iran in 2017. He is currently a member of Applied Sciences Faculty of Malek Ashtar University of Technology. His researches are in the fields of laser and optic.



**Mohammad Mahdi Moslem** was born in 1998. He received his master's degree in Electro-Optics from Malek Ashtar University of Technology, ShahinShar, Iran.



**Nabiollah Azarpoor** was born in 1997. He received a bachelor's degree in Optic and laser engineering from Urmia University of Technology and master's degree in Electro-Optics from Malek Ashtar University of Technology, ShahinShar, Iran. He is interested in imaging systems, adaptive optics, and design of optical systems.